Title: Rhoptry neck protein RON2 forms a complex with microneme protein AMA1 in *Plasmodium falciparum* merozoites

Jun Cao[a,b], Osamu Kaneko[a,c,*], Amporn Thongkukiatkul[d], Mayumi Tachibana[a], Hitoshi Otsuki[a], Qi Gao[b], Takafumi Tsuboi[e,f], Motomi Torii[a]

[a] *Department of Molecular Parasitology, Ehime University Graduate School of Medicine, Shitsukawa, Toon, Ehime 791-0295, Japan*

[b] *Malaria Department, Jiangsu Institute of Parasitic Diseases, Meiyuan, Wuxi, Jiangsu 214064, People's Republic of China*

[c] *Department of Protozoology, Institute of Tropical Medicine (NEKKEN), Nagasaki University, Sakamoto, Nagasaki 852-8523, Japan*

[d] *Department of Biology, Faculty of Science, Burapha University, Chonburi 20131, Thailand*

[e] *Cell-Free Science and Technology Research Center, Ehime University, Matsuyama, Ehime 790-8577, Japan*

[f] *Venture Business Laboratory, Ehime University, Matsuyama, Ehime 790-8577, Japan*

Abbreviations: aa, amino acid(s); Ab, antibody; AMA1, apical membrane antigen 1; GST, Glutathione S transferase; PBS, phosphate-buffered saline; PCR, polymerase chain reaction; RON, rhoptry neck protein.

* Corresponding author: Tel.: (+81) 95 819 7838; Fax: (+81) 95 819 7805; E-mail address: okaneko@nagasaki-u.ac.jp

Sequence data from this article have been deposited with the GenBank™/EMBL/DDBJ databases under accession numbers AB444588–AB444592.

Abstract

Erythrocyte invasion is an essential step in the establishment of host infection by malaria parasites, and is a major target of intervention strategies that attempt to control the disease. Recent proteome analysis of the closely-related apicomplexan parasite, *Toxoplasma gondii*, revealed a panel of novel proteins (RONs) located at the neck portion of the rhoptries. Three of these proteins, RON2, RON4, and RON5 have been shown to form a complex with the microneme protein Apical Membrane Protein 1 (AMA1). This complex, termed the Moving Junction complex, localizes at the interface of the parasite and the host cell during the invasion process. Here we characterized a RON2 ortholog in *Plasmodium falciparum*. *Pf*RON2 transcription peaked at the mature schizont stage and was expressed at the neck portion of the rhoptry in the merozoite. Co-immunoprecipitation of *Pf*RON2, *Pf*RON4 and *Pf*AMA1 indicated that the complex formation is conserved between *T. gondii* and *P. falciparum*, suggesting that co-operative function of the rhoptry and microneme proteins is a common mechanism in apicomplexan parasites during host cell invasion. *Pf*RON2 possesses a region displaying homology with the rhoptry body protein *Pf*RhopH1/Clag, a component of the RhopH complex. However, here we present co-immunoprecipitation studies which suggest that *Pf*RON2 is not a component of the RhopH complex and has an independent role. Nucleotide polymorphism analysis suggested that *Pf*RON2 was under diversifying selective pressure. This evidence suggests that RON2 appears to have a fundamental role in host cell invasion by apicomplexan parasites, and is a potential target for malaria intervention strategies.

Keywords: AMA1; erythrocyte invasion; merozoite; *Plasmodium falciparum*; rhoptry

1. Introduction

Malaria is one of the most prevalent and deadly global infectious diseases, more than half of the world's population is at the risk of infection, and over 300 million people develop clinical disease each year of which 2 million are fatal [1]. Clinical malaria results from the replication of protozoan parasites of the genus *Plasmodium* in the circulating erythrocytes of the host. During the time between release from a rupturing mature schizont-infected erythrocyte and invasion of new erythrocytes, merozoites are transiently exposed in the circulation, and are thus potentially vulnerable to attack by preventive measures based upon immunological or biochemical methods. To design such tools, it is important to understand the molecular composition of the merozoite and the structure-function makeup of the molecular interactions that occur as the merozoite recognizes and gains entry into a host cell.

Like most apicomplexan parasites, the malaria merozoite invades host cells via a multistep process initiated by reversible binding to the erythrocyte surface. Subsequently, a high affinity attachment occurs between the apical end of the merozoite and the host cell, followed by the movement of the junctional adhesion zone (moving junction) around the merozoite toward its posterior pole. Finally the merozoite invaginates into the erythrocyte by forming a nascent parasitophorous vacuole [2]. The moving junction is one of the most distinctive features of apicomplexan invasion and was first observed in *Plasmodium* species in the late 1970s [3], but the molecular nature of its structure remains unresolved.

Recent studies in *Toxoplasma gondii* suggest that host cell invasion involves protein

discharge from at least two apical secretory organelles, the micronemes and rhoptries, based on the observation that a microneme protein, Apical Membrane Protein 1 (AMA1), forms a complex with three rhoptry neck (RON) proteins: RON2, RON4 and Ts4705 (RON5) [4 – 6]. These proteins have predicted orthologs in *P. falciparum*, and the RON4 ortholog has been reported to associate with *Pf*AMA1 [7] and to be localized at the moving junction [8], suggesting that the complex (and likely its function) is conserved between *T. gondii* and *P. falciparum* [7]. Attempts to knock-out the AMA1 gene locus were unsuccessful in both *Plasmodium* [9] and *T. gondii* [10], and the conditional reduction of *Tg*AMA1 expression severely impaired the cell invasion ability of *T. gondii* [11], indicating AMA1 has an essential function. The conservation of the RON proteins among apicomplexan parasites suggest that their functions and protein interactions are also conserved in the biology of host cell invasion. However, in *Plasmodium*, the details of this complex have yet to be fully characterized. In this study, to better understand the moving junction complex formation in *Plasmodium*, we sought to characterize *Pf*RON2 and determine the nature of its interaction with *Pf*RON4 and *Pf*AMA1.

2. Materials and methods

2.1 Malaria parasites

P. falciparum cloned lines 3D7, HB3, Dd2, 7G8, FVO, and D10 were maintained *in vitro*, essentially as previously described [12].

2.2. DNA and RNA isolation

Genomic DNA (gDNA) was isolated from *P. falciparum* using IsoQuick™ (Orca Research Inc., Bothell, WA). To determine transcription levels throughout the asexual stages, schizonts were purified by differential centrifugation on a 70%/40% Percoll-sorbitol gradient, after which released merozoites were allowed to invade uninfected erythrocytes for 4 hours before the clearance of all remaining schizonts using 5% D-sorbitol. Fractions of the culture were harvested immediately and 24 hours later, and then at 6 hour intervals thereafter. Total RNA was isolated from parasite-infected erythrocytes stored at –20°C in RNA*later*™ (Qiagen, Valencia, CA), using the RNeasy Mini Kit (Qiagen). Following DNase treatment, complementary DNA (cDNA) was generated with random hexamers using an Omniscript Reverse Transcription Kit (Qiagen).

2.3. Polymerase chain reaction (PCR) amplification and sequencing

A TBLASTN search was performed against the *P. falciparum* genome database (3D7 parasite line) via PlasmoDB website (http://www.plasmodb.org/) [13] using the *Tg*RON2 amino acid sequence as a query. To evaluate the polymorphism of *Pf*RON2, five pairs of overlapping primers were used for PCR amplification from HB3, FVO, Dd2, D10, and 7G8 parasite lines, and sequences were determined by direct sequencing of the PCR-amplified DNA fragments using an ABI PRISM® 3100-*Avant* Genetic Analyzer (Applied Biosystems, Foster City, CA). Oligonucleotides used were as follows: fRON2.F2 (5'-GATTCCAATAATTATAATTCTGATAATG-3') and fRON2.R2 (5'-CGTAAAATATTCATTATATGAAAGATATGC-3'), fRON2.F3 (5'-GCATTAGGAGAACTTGTTGAACCA-3') and fRON2.R3 (5'-CATAATATCTAAATAGGTTTTTGCTGAC-3'), fRON2.F4 (5'-GGATTAGTATTTTTATATGCAATGATTG-3') and fRON2.R4

(5'-GTTATTTTCTAATAAATGTTTACTATCTTC-3'), fRON2.F5 (5'-GATAAATGGGATCAATTTATAAATAAGG-3') and fRON2.R5 (5'-GCTAGCTACTGGTCCTGCACCT-3'), and fRON2.F6 (5'-ATGCAATTACCTTACTTAAGTCAAATG-3') and fRON2.R6 (5'-ATATAAAATGAAAATAACAGAAAAGGTTATG-3')

2.4. Quantification of pfron2 *transcripts*

Transcription of *ron2* was evaluated in the HB3 parasite line by real-time reverse transcription (RT)-PCR using a QuantiTect SYBR Green PCR Kit (Qiagen) and a LightCycler System (Roche, Basel, Switzerland). As a control, transcription of *ama1* and *rhoph2* was also evaluated. Oligonucleotides used were as follows: fRON2.qF (5'-CAGAACTAAGCAAACATGTAAAACATG-3') and fRON2.qR (5'-GTATAACGCCTTGCTCATTTCCTG-3') for *pfron2* (product size is 133 bp); fAMA1.qF (5'-GGAAGAGGACAGAATTATTGGGAAC-3') and fAMA1.qR (5'-CCTGAATCTTCTTGTTGGTATGTATG-3') for *pfama1* (product size is 137 bp); fRhopH2.qF (5'-GTAACAACACTTACTAAGGCAGACT-3') and fRhopH2.qR (5'-GTACAAAGCTACAATATTGTTAGATCT-3') for *pfrhoph2* (product size is 210 bp). The same oligonucleotides were used to PCR-amplify DNA fragments to be ligated into the pGEM-T Easy® plasmid (Promega, Madison, WI) which was used to make a standard curve to evaluate the copy number of each transcript.

2.5. Antibodies

A DNA fragment encoding amino acid positions (aa) 21 – 98 of *Pf*RON2 was PCR-amplified from *P. falciparum* 3D7 gDNA and ligated into pEU-E01GST-N2, an expression plasmid with N-terminal glutathione S transferase (GST)-tag followed by a PreScission Protease cleavage site, designed specifically for the wheat germ cell-free protein expression system (CellFree Sciences Co., Ltd., Matsuyama, Japan) [14], to produce recombinant GST-fused fRON2N protein (GST-fRON2N). Oligonucleotides used in the PCR amplification were fRON2.SalF1 (5'-GTCGACTCAGAACTAAGCAAACATGTAAAACATG-3') and fRON2.SalR1 (5'-GTCGACCCCATTATTCATTTCACTACCAGGA-3') (*Sal*I restriction sites are underlined). Produced GST-fRON2N was captured using a glutathione-Sepharose 4B column and eluted with 10 mM reduced gluthathione, pH8.0. To generate anti-*Pf*RON2 sera, BALB/c mice were immunized subcutaneously with 20 μg of purified GST-fRON2N emulsified with Freund's adjuvant. A Japanese white rabbit was immunized subcutaneously with 500 μg of purified GST-fRON2N with Freund's adjuvant for the first time, followed by 250 μg thereafter. All immunizations were done 4 times at 3 week intervals, prior to collection of antisera. Rabbit anti-*Pf*RhopH2 serum was obtained from I. Ling (National Institute for Medical Research, UK) [15], Rabbit anti-*Pf*AMA1 serum was obtained from C. Long (National Institute of Health, USA), and mouse monoclonal anti-*Pf*RON4 antibody (Ab; 26C64F12) was obtained from J.-F. Dubremetz (Université de Montpellier 2, France) [7]. Rabbit anti-Clag3.1 serum was as previously described [16].

2.6. SDS-PAGE and Western blot analysis

The recombinant protein, GST-fRON2N, was digested with a PreScission Protease at 4°C overnight before analysis. Triton X-100 extracts of *P. falciparum* or recombinant proteins

were dissolved in SDS-PAGE loading buffer, incubated at 100°C for 3 min, and subjected to electrophoresis under reducing conditions on a 5–20% polyacrylamide gel (ATTO, Japan). Proteins were then transferred to a 0.22 μm PVDF membrane (BioRad, Hercules, CA). The proteins were immunostained with antisera followed by horseradish peroxidase-conjugated secondary Ab (Biosource Int., Camarillo, CA) and visualized with Immobilon™ Western Chemiluminescent HRP Substrate (Millipore, Billerica, MA) on RX-U film (Fuji, Japan). The relative molecular sizes of the parasite-encoded proteins were calculated by reference to molecular size standards (BioRad).

2.7. Immunoprecipitation

Immunoprecipitation was carried out as previously described [17]. Briefly, proteins were extracted from late schizont parasite pellets by 1% Triton X-100 treatment in phosphate-buffered saline (PBS) containing cOmplete Proteinase Inhibitor Cocktail Tablets (Roche). Supernatants (50 μl) were pre-incubated at 4°C for 1 hour with 20 μl of 50% protein G-conjugated beads (GammaBind Plus Sepharose; GE Healthcare) in NETT buffer (50 mM Tris–HCl, 0.15 M NaCl, 1 mM EDTA, and 0.5% Triton X-100) supplemented with 0.5% BSA (fraction V; Sigma-Aldrich). Recovered supernatants were incubated with rabbit antisera (anti-*Pf*RON2, anti-*Pf*AMA1, or anti-*Pf*RhopH2) or mouse anti-*Pf*RON4 Ab with gentle rotation at 4°C for 2 hours and then 20 μl of 50% protein G-conjugated beads were added. After 1 hour incubation at 4°C, the beads were washed once with NETT-0.5% BSA, once with NETT, once with high-salt NETT (0.5 M NaCl), once with NETT, and once with low-salt NETT (0.05 M NaCl and 0.17% Triton X-100). Finally, proteins were extracted from the protein G-conjugated beads by incubation with SDS-PAGE reducing loading buffer at 100°C for 3 min. Supernatants were collected for Western blot analysis.

2.8. Indirect immunofluorescence assay

Thin smears of schizont-enriched *P. falciparum*-infected erythrocytes (Dd2 parasite line) were prepared on glass slides and stored at –80ºC. The smears were thawed, formaldehyde-fixed, and preincubated with PBS containing 5% non-fat milk at 37ºC for 30 min. They were then incubated with antisera at 37ºC for 1 hour, followed by fluorescein isothiocyanate (FITC)-conjugated goat anti-(IgG and IgM) secondary Ab (Jackson ImmunoResearch Laboratories, West Grove, PA) and Alexa546-conjugated goat anti-(IgG and IgM) secondary Ab (Invitrogen, Carlsbad, CA) at 37ºC for 30 min. Nuclei were stained with 4',6-diamidino-2-phenylindole (DAPI). Slides were mounted in ProLong Gold antifade reagent (Invitrogen) and viewed under oil-immersion. High resolution image-capture and processing were performed using a confocal scanning laser microscope (LSM5 PASCAL; Carl Zeiss MicroImaging, Thornwood, NY). Images were processed in Adobe Photoshop (Adobe Systems Inc., San José, CA).

2.9. Immunoelectron microscopy

Parasites were fixed for 15 min on ice in a mixture of 1% paraformaldehyde–0.1% glutaraldehyde in 0.1 M phosphate buffer (pH 7.4). Fixed specimens were washed, dehydrated, and embedded in LR White resin (Polysciences, Inc., Warrington, PA) as previously described [18, 19]. Thin sections were blocked at 37°C for 30 min in PBS containing 5% non-fat milk and 0.01% Tween 20 (PBS-MT). Grids were then incubated at 4°C overnight with mouse anti-*Pf*RON2 or control sera in PBS-MT. After washing with PBS containing 10% BlockAce (Yukijirushi, Sapporo, Japan) and 0.01% Tween 20 (PBS-BT), the

grids were incubated at 37°C for 1 hour with goat anti-mouse IgG conjugated to 10 nm gold particles (Amersham Life Science, Arlington, IL) diluted 1:20 in PBS-MT, rinsed with PBS-BT, and fixed on ice for 10 min in 2.5% glutaraldehyde to stabilize the gold. Then the grids were rinsed with distilled water, dried, and stained with uranyl acetate and lead citrate. Samples were examined with a transmission electron microscope (JEM-1230; JEOL Ltd., Tokyo, Japan).

2.10. Primary structure analysis of the protein

Signal peptide sequence was evaluated by SignalP3.0 [20]. Transmembrane region was evaluated by TMpred [21] and TMHMM2.0 [22]. Low complexity region was evaluated by Globplot 2.3 [23]. Amino acid sequence alignment was generated by MUSCLE [24].

2.11. Statistical analysis

Number of nonsynonymous substitutions over numbers of nonsynonymous sites (d_N), number of synonymous substitutions over numbers of synonymous sites (d_S), and their standard errors were computed using the Nei-Gojobori method with Jukes-Cantor correction implemented in MEGA 4.0.1 [25]. Standard errors were estimated using the bootstrap method with 500 replications. The statistical difference between d_N and d_S was tested using a one-tail Z-test with 500 bootstrap pseudosamples.

3. Results

3.1. RON2 orthologs of apicomplexan parasites

Using *Tg*RON2 as a query in BLAST analyses [26], and similar analyses using the predicted orthologs thus identified, we found RON2 orthologs in *P. falciparum* (*Pf*RON2; PF14_0495, PlasmoDB), *P. yoelii* 17XNL strain (*Py*RON2; PY06813, TIGR), *P. knowlesi* H strain (*Pk*RON2; PKH_125430 or PK14_2335w, Sanger Centre), and *P. vivax* Sal-I strain (*Pv*RON2; Pv117880, TIGR), *P. berghei* (*Pb*RON2; Contig5108), *P. chabaudi* (*Pch*RON2; Contig882.0), *Theileria annulata* (*Ta*RON2; Fig. S1A, TA19445 and TA19390, Sanger Centre [27]), *Theileria parva* (*Tp*RON2; Fig. S1B, TP01_0014, TIGR [28]), and *Babesia bigemina* (*Bbig*RON2; Fig. S1C, Contig3449, Sanger Centre). The RON2 were fragmented in the *P. berghei*, *P. chabaudi*, *T. annulata*, and *T. parva* genome nucleotide sequence databases, and full-length versions were constructed (supplementary Table S1).

*3.2.*Pf*RON2 protein structure and similarity to RhopH1/Clag proteins*

The full-length *Pf*RON2 protein consists of 2189 residues with a putative signal peptide sequence at its N-terminus from amino acid positions (aa) 1 to 20. An interspecies variable region (aa 55 – 878), exhibiting low complexity and many repeats [23], was identified by comparing 6 *Plasmodium* RON2 amino acid sequences (Fig. 1 and Fig. S2). A BLASTP search using the conserved region of *Pf*RON2 (aa 879 – 2189) as a query identified *P. vivax* RhopH1/Clag homolog (XP_001616939.1, aa 251 – 394; E = 0.001) as possessing homology with *Pf*RON2 aa 1105 – 1259. A Position-Specific Iterated BLAST search using *Pf*RON2 aa 1105 – 1259 as a query converged at iteration 3 and indentified most of the RhopH1/Clag genes in *Plasmodium* species. Alignment of RhopH1/Clag with RON2 from multiple genera identifies a predicted globular domain that is likely stabilized by disulfide bonds between 4 conserved Cys residues (Fig. 2). Three transmembrane regions were predicted by TMpred,

however TMHMM2.0 predicted only a single transmembrane region for all *Plasmodium* RON2 orthologs assessed.. Interestingly, TMpred predicted a putative transmembrane region in the region conserved between RhopH1/Clag and RON2 (Fig. 2). Because RhopH1/Clag is a component of a soluble protein complex, we considered that these predicted transmembrane regions in RhopH1/Clag and RON2 constitute a likely hydrophobic region buried within a globular domain. Another predicted transmembrane region at aa 1114 – 1133 in *Pf*RON2 is also possibly hydrophobic region buried within a globular domain. TMpred considers the observation that there is an overrepresentation of positively charged amino acid residues in the cytoplasmic loops of the transmembrane protein [21], which is a likely explanation for this discrepancy.

3.3. Pf*RON2 transcription peaks at the schizont stage*

To determine the transcription pattern in the asexual stages of the parasite life-cycle, quantitative RT-PCR was performed on the HB3 parasite line prepared from a synchronized culture harvested at 6 hour intervals. Both RON2 and AMA1 transcriptions were seen to peak around 36 – 40 hours after invasion, when parasites were in the schizont stage. AMA1 showed a broader and flatter transcription peak than RON2 (Fig. 3). Transcriptome data compiled in the PlasmoDB website [13, 29] also indicated a milder wave crest of AMA1 transcripts compared with RON2.

3.4. Complex formation of Pf*RON2,* Pf*RON4, and* Pf*AMA1*

Mouse and rabbit anti-*Pf*RON2 sera were generated using recombinant GST-fRON2N. Firstly, we evaluated the reactivity of anti-*Pf*RON2 sera by Western blot using recombinant

proteins. Both antisera recognized the fRON2N component of the recombinant protein after cleavage (Fig. S3, filled arrows). Cleaved 26.4-kDa GST component (Fig. S3, arrowheads) and 46-kDa GST-fused PreScission protease (Fig. S3, unfilled arrow) were also recognized by these Abs.

Secondly, we evaluated the reactivity of these sera against native RON2 proteins extracted from schizont stage *P. falciparum* (HB3 line) by Western blot analysis. Both antisera reacted with a band slightly larger than 250 kDa (Fig. 4A, arrows), which is similar to the predicted molecular weight of *Pf*RON2 after exclusion of the putative signal peptide sequence (247 kDa). An 80-kDa band was detected by both mouse and rabbit antisera in HB3 extract, for which the exact identity is not known, but a possible processed product of *Pf*RON2. A 55-kDa band detected with rabbit antiserum was also detected with preimmune serum, suggesting that this band was unrelated to *Pf*RON2. A 35-kDa band was detected with mouse antiserum but not with rabbit antiserum, suggesting that it is also unrelated to RON2.

To evaluate the interaction between *Pf*RON2, *Pf*RON4, and *Pf*AMA1, we performed immunoblotting against immunoprecipitated materials from mature schizont-rich parasite extracts (Fig. 5). We found that RON2 was detected in the precipitated fraction using anti-*Pf*AMA1 or anti-*Pf*RON4. In the reciprocal experiment, *Pf*AMA1 and *Pf*RON4 were also detected in the precipitated fraction of anti-*Pf*RON2 serum. Although it is theoretically possible that such immunoprecipitated fractions contained the *Pf*RON2-*Pf*RON4, *Pf*RON2-*Pf*AMA1, and *Pf*RON4-*Pf*AMA1 dimeric complexes as appropriate to the primary antibody, considering that these 3 proteins are distinct molecules that do not possess any similarity each other, this specific co-immunoprecipitation suggests complex formation among *Pf*RON2, *Pf*RON4, and *Pf*AMA1 in *P. falciparum*. The fact that both the 83-kDa proform and the 66-kDa processed form were co-precipitated with *Pf*RON2 indicated that a region responsible for complex formation was located in the 66-kDa form of AMA1 [30].

Neither of these was detected in the anti-RhopH2 immunoprecipitate, thereby excluding not only the possibility of *Pf*RON2 involvement in the RhopH complex, but also potential carryover due to insufficient or inadequate washing steps.

3.5. RON2 is expressed at the rhoptry neck of Plasmodium *merozoites*

Dual labeling indirect immunofluorescent assay was performed using anti-*Pf*RON2 with either anti-*Pf*AMA1 (microneme marker), anti-Clag3.1 (rhoptry body marker), or anti-*Pf*RON4 (rhoptry neck marker) antibodies in order to determine the sub-cellular location of *Pf*RON2 in *P. falciparum* (Fig. 6). In segmented schizonts, RON2 antisera produced a punctate pattern of fluorescence and each developing merozoite showed a single small punctate *Pf*RON2-positive signal located at the apical end. Although some parts of the *Pf*RON2 signal overlapped with microneme protein AMA1 and rhoptry body protein Clag3.1, it did not colocalize well with those markers, whereas complete colocalization was observed with the rhoptry neck marker *Pf*RON4.

Immunoelectron microscopy was carried out to determine the precise localization of the protein. *Pf*RON2 was detected in the neck portion of the pear-shaped rhoptries in segmented schizonts (Fig. 7). Thus *Pf*RON2 is seen to compartmentalize in the rhoptry neck.

3.6. Potential positive diversifying selection on Pf*RON2*

To evaluate the polymorphic nature of *Pf*RON2, we sequenced the *pfron2* nucleotide sequence (2459 – 6570), excluding the 5' low complexity region, in 5 *P. falciparum* parasite lines and compared them with the sequence from the genome database (3D7 line). A total of 5 nonsynonymous nucleotide substitutions were observed at nucleotide positions 2615, 2710,

2914, 4391 and 4392, resulting 4 amino acid substitutions (Table 1). An excess of nonsynonymous substitutions (d_N = 0.0007 ± 0.0003) over synonymous substitutions (d_S = 0.0002 ± 0.0002) was detected (P = 0.0333), indicating *Pf*RON2 is subject to positive diversifying selection.

4. Discussion

In this study, we characterized *P. falciparum* RON2 for its protein structure, transcription profiles, intracellular localization, and complex formation with *Pf*RON4 and *Pf*AMA1.

*Pf*RON2 possesses a region harboring homology with another rhoptry protein RhopH1/Clag, a component of the RhopH complex that possesses erythrocyte binding ability [16, 31, 32]. Co-immunoprecipitation showed that *Pf*RON2 does not form a complex with RhopH2, suggesting that *Pf*RON2 is unlikely to be a component of the RhopH complex. Because RON2 orthologs can be found in other apicomplexan parasites and RhopH1/Clag is found only in *Plasmodium* species, RhopH1/Clag probably evolved via acquisition of a conserved functional domain from RON2 during its generation in *Plasmodium* species. Thus, this homologous region may have a common function between these two complexes. The sequence of *Tg*RON2 deposited to the database (GenBank accession number DQ096563) only possesses the C-terminal half of the conserved region between RON2 and RhopH1/Clag. By comparing *Tg*RON2 gDNA and cDNA sequences, we noticed that intron 3 is relatively large (2272 bp) and contains a potential sequence encoding the N-terminal portion of the conserved region. Thus it is possible that there is another alternatively spliced transcript encoding the full length of the conserved region. Alternatively, it is also possible that this region represents an ancient vestigial exon.

Interestingly, we could readily detect complex formation between AMA1 and RON proteins in the extract obtained from mature schizont-rich parasites, suggesting that complex formation had already occurred at the schizont stage likely at the apical end upon secretion of RON proteins from rhoptry and AMA1 from microneme. This is in contrast to the other apicomplexa parasite *T. gondii*, in which the AMA1-RON complex was proposed to form at the initial contact with the host cell. The precise timing of the complex formation is not clear, but may vary depending on the parasite species. Among RON proteins characterized thus far, only *Tg*RON4 was visualized to locate at the moving junction during cell invasion. Whether *Pf*RON2 and *Pf*RON4 locate at the moving junction and whether the complex remains intact during cell invasion are still need to be clarified. We found that *Pf*RON2 degraded more rapidly than *Pf*RON4 after extraction (Fig. S4), which may explain the previous observation by Alexander et al. (2006), who did not detect *Pf*RON2 in the immunoprecipitant with anti-*Pf*AMA1 Ab [7].

The association between the 83-kDa proform of *Pf*AMA1 with RON proteins raises the possibility that the processing of *Pf*AMA1 from the 83-kDa form to 66-kDa form occurs not only in the microneme, as previously proposed [33], but also on the apical tip of the merozoite after release from the microneme in mature schizonts. If this is the case, it is not clear whether this AMA1 processing occurs after complex formation with RON proteins or is mainly achieved prior to this. However, it is formally possible that disruption of the different intracellular microorganelles during the experimental procedure resulted an artificial complex formation of *Pf*AMA1 proform, for which further studies are required.

Due to the fact that *P. falciparum* AMA1 exhibits relatively high polymorphism between lines, which is considered to be generated by positive diversifying selection under the human immune pressure, we evaluated the polymorphic nature of *Pf*RON2. Although the level of polymorphism of RON2 is not high, the fact that $d_N > d_S$ suggests that positive diversifying

selection does indeed act on RON2. Three types of amino acid substitutions found at aa 1464 (Asp, Glu, and Gly) suggests that this particular site is under diversifying selection and is possibly to be exposed to host immunity. Thus, *Pf*RON2 not only appears to have an important role in host cell invasion by apicomplexan parasites, but also is a potential target for malaria intervention strategies.

Acknowledgements

We thank N Iyoku for her expertise, I Ling for anti-*Pf*RhopH2 serum, C Long for anti-*Pf*AMA1 serum, anti-*Pf*RON4 antibody (26C64F12) for J-F Dubremetz, and R Culleton for critical reading. Preliminary sequence data of *P. knowlesi, P. berghei, P. chabaudi,* and *B. bigemina* were produced by the corresponding groups at the Sanger Institute website at http://www.sanger.ac.uk/. Preliminary sequence data of *P. vivax* was produced at the Institute for Genomic Research website at http://www.tigr.org. This work was supported in part by Grants-in-Aid for Scientific Research 17590372 and 17406009 (to OK) from the Ministry of Education, Culture, Sports, Science and Technology, Japan. JC acknowledges the support of National Natural Science Foundation of China 30700695.

References

[1] Snow RW, Guerra CA, Noor AM, Myint HY, Hay SI. The global distribution of clinical episodes of *Plasmodium falciparum* malaria. Nature 2005;434:214–7.

[2] Kaneko O. Erythrocyte invasion: vocabulary and grammar of the *Plasmodium* rhoptry. Parasitol Int 2007;56:255–62.

[3] Aikawa M, Miller LH, Johnson J, Rabbege J. Erythrocyte entry by malarial parasites. A moving junction between erythrocyte and parasite. J Cell Biol 1978;77:72–82.

[4] Boothroyd JC, Dubremetz JF. Kiss and spit: the dual roles of *Toxoplasma* rhoptries. Nat Rev Microbiol 2008;6:79–88.

[5] Alexander DL, Mital J, Ward GE, Bradley P, Boothroyd JC. Identification of the moving junction complex of *Toxoplasma gondii*: a collaboration between distinct secretory organelles. PLoS Pathog 2005;1:e17.

[6] Lebrun M, Michelin A, El Hajj H, Poncet J, Bradley PJ, Vial H, *et al.* The rhoptry neck protein RON4 re-localizes at the moving junction during *Toxoplasma gondii* invasion. Cell Microbiol 2005;7:1823–33.

[7] Alexander DL, Arastu-Kapur S, Dubremetz JF, Boothroyd JC. *Plasmodium falciparum* AMA1 binds a rhoptry neck protein homologous to TgRON4, a component of the moving junction in *Toxoplasma gondii*. Eukaryot Cell 2006;5:1169–73.

[8] Baum J, Tonkin CJ, Paul AS, Rug M, Smith BJ, Gould SB, et al. A malaria parasite formin regulates actin polymerization and localizes to the parasite-erythrocyte moving junction during invasion. Cell Host Microbe 2008;3:188–98.

[9] Triglia T, Healer J, Caruana SR, нodder AN, Anders RF, Crabb BS, et al. Apical membrane antigen 1 plays a central role in erythrocyte invasion by *Plasmodium* species. Mol Microbiol. 2000;38:706–18.

[10] Hehl AB, Lekutis C, Grigg ME, Bradley PJ, Dubremetz JF, Ortega-Barria E, et al. *Toxoplasma gondii* homologue of *Plasmodium* apical membrane antigen 1 is involved in invasion of host cells. Infect Immun 2000;68:7078–86.

[11] Mital J, Meissner M, Soldati D, Ward GE. Conditional expression of *Toxoplasma gondii* apical membrane antigen-1 (TgAMA1) demonstrates that TgAMA1 plays a critical role in host cell invasion. Mol Biol Cell 2005;16:4341–9.

[12] Trager W, Jensen JB. Human malaria parasites in continuous culture. Science 1976;193:673–5.

[13] Bahl A, Brunk B, Crabtree J, Fraunholz MJ, Gajria B, Grant GR, et al. PlasmoDB: the *Plasmodium* genome resource. A database integrating experimental and computational data. Nucleic Acids Res 2003;31:212–5.

[14] Tsuboi T, Takeo S, Iriko H, Jin L, Tsuchimochi M, Matsuda S, et al. The wheat germ cell-free based production of malaria proteins for discovery of novel vaccine candidates. Infect Immun 2008;76:1702–8.

[15] Ling IT, Kaneko O, Narum DL, Tsuboi T, Howell S, Taylor HM, et al. Characterisation of the *rhoph2* gene of *Plasmodium falciparum* and *Plasmodium yoelii*. Mol Biochem Parasitol 2003;127:47–57.

[16] Kaneko O, Yim Lim BY, Iriko H, Ling IT, Otsuki H, Grainger M, et al. Apical expression of three RhopH1/Clag proteins as components of the *Plasmodium falciparum* RhopH complex. Mol Biochem Parasitol 2005;143:20–8.

[17] Kaneko O, Fidock DA, Schwartz OM, Miller LH. Disruption of the C-terminal region of EBA-175 in the Dd2/Nm clone of *Plasmodium falciparum* does not affect erythrocyte invasion. Mol Biochem Parasitol 2000;110:135–46.

[18] Torii M, Adams JH, Miller LH, Aikawa M. Release of merozoite dense granules during erythrocyte invasion by *Plasmodium knowlesi*. Infect Immun 1989;57:3230–3.

[19] Aikawa M, Atkinson CT. Immunoelectron microscopy of parasites. Adv Parasitol 1990;29:151–214.

[20] Bendtsen JD, Nielsen H, von Heijne G, Brunak S. Improved prediction of signal peptides: SignalP 3.0. J Mol Biol 2004:340;783–95.

[21] Hofmann K, Stoffel W. TMbase - A database of membrane spanning proteins segments. Biol Chem. Hoppe-Seyler 1993;374:166.

[22] Krogh A, Larsson B, von Heijne G, Sonnhammer EL. Predicting transmembrane protein topology with a hidden Markov model: application to complete genomes. J Mol Biol 2001:305;567–80.

[23] Linding R, Russell RB, Neduva V, Gibson TJ. GlobPlot: Exploring protein sequences for globularity and disorder. Nucleic Acids Res 2003;31:3701–8.

[24] Edgar RC. MUSCLE: multiple sequence alignment with high accuracy and high throughput. Nucleic Acids Res 2004;32,1792–7.

[25] Tamura K, Dudley J, Nei M, Kumar S. MEGA4: Molecular Evolutionary Genetics Analysis (MEGA) software version 4.0. Mol Biol Evol 2007;24:1596–9.

[26] Altschul SF, Madden TL, Schäffer AA, Zhang J, Zhang Z, Miller W, et al. Gapped BLAST and PSI-BLAST: a new generation of protein database search programs. Nucleic Acids Res 1997;25:3389-3402.

[27] Pain A, Renauld H, Berriman M, Murphy L, Yeats CA, Weir W, et al. Genome of the host-cell transforming parasite *Theileria annulata* compared with *T. parva*. Science 2005;309:131–3.

[28] Gardner MJ, Bishop R, Shah T, de Villiers EP, Carlton JM, Hall N, et al. Genome sequence of *Theileria parva*, a bovine pathogen that transforms lymphocytes. Science 2005;309:134–7.

[29] Le Roch KG, Zhou Y, Blair PL, et al. Discovery of gene function by expression profiling of the malaria parasite life cycle. Science 2003;301:1503–8.

[30] Howell SA, Withers-Martinez C, Kocken CH, Thomas AW, Blackman MJ. Proteolytic processing and primary structure of *Plasmodium falciparum* apical membrane antigen-1. J Biol Chem 2001;276:31311–20.

[31] Ghoneim A, Kaneko O, Tsuboi T, Torii M. The *Plasmodium falciparum* RhopH2 promoter and first 24 amino acids are sufficient to target proteins to the rhoptries. Parasitol Int 2007;56:31-43.

[32] Rungruang T, Kaneko O, Murakami Y, Tsuboi T, Hamamoto H, Akimitsu N, et al. Erythrocyte surface glycosylphosphatidyl inositol anchored receptor for the malaria parasite. Mol Biochem Parasitol 2005;140:13–21.

[33] Healer J, Triglia T, Hodder AN, Gemmill AW, Cowman AF. Functional analysis of *Plasmodium falciparum* apical membrane antigen 1 utilizing interspecies domains. Infect Immun 2005;73:2444–51.

Figure legends

Figure 1. Schematic representation of *Pf*RON2. S and TM indicate putative signal peptide (aa 1 – 20) and transmembrane sequences, respectively. The shaded box indicates an interspecies variable region. Vertical red bars indicate conserved Cys residues among orthologous sequences. Homologous region between RhopH1/Clag and RON2 is indicated by a yellow box. The region used to generate anti-*Pf*RON2 sera (α-*Pf*RON2) and the region sequenced in the laboratory lines (sequencing) are indicated. Asterisks indicate polymorphic sites.

Figure 2. Amino acid alignment of *Plasmodium* RON2 and RhopH1/Clag. Alignment was generated by MUSCLE [24] with manual correction. "*" indicates that the residues in that column are identical in all sequences in the alignment. ":" indicates conserved substitutions and "." indicates semi-conserved substitutions. In addition to 9 RON2 sequences, *P. falciparum* Clag2 (AAC71977), Clag9 (CAD52032), *P. yoelii* RhopH1A (BAB70675),

RhopH1AP (BAB70677), and *Pv*RhopH1 (contig 1047) were used to generate the alignment. Cys residues are highlighted in red. The region possessing homology between RhopH1/Clag and RON2 as identified by BLASTP is indicated by the bar under the alignment.

Figure 3. Transcriptional analysis by quantitative RT-PCR of *pfrhoph2, pfron2,* and *pfama1* genes during blood stages of *P. falciparum* (HB3 line). *Y*-axis indicates copy number of each transcript detected per 1000 parasites. Similar results were observed in 3 independent experiments (data not shown).

Figure 4. Western blot analysis of antisera against native parasite proteins. (A) Schizont-enriched parasite extracts were stained by rabbit preimmune serum, (Rab preimmune), rabbit anti-*Pf*RON2 (Rab α-*Pf*RON2), mouse anti-fRON2N (Mo α-*Pf*RON2), and Abs against GST (Mo α-GST) or *Pf*AMA1 (Mo α-*Pf*AMA1) under both reducing and non-reducing conditions. Both mouse and rabbit anti-*Pf*RON2 sera detected a band slightly larger than 250 kDa. (B) Western blot of schizont-enriched parasite extracts from 3 different *P. falciparum* lines, Dd2, 3D7, and HB3 with mouse anti-fRON2N serum. Arrows indicate predicted *Pf*RON2 bands.

Figure 5. *Pf*RON2 is co-precipitated with *Pf*RON4 and *Pf*AMA1. Schizont-rich parasite Triton X-100 extracts (*Pf* Tx extract) were immunoprecipitated (IP) with rabbit sera against *Pf*RhopH2 (α-*Pf*RhopH2), *Pf*RON2 (α-*Pf*RON2), *Pf*AMA1 (α-*Pf*AMA1) or mouse monoclonal Ab against *Pf*RON4 (α-*Pf*RON4), then stained against *Pf*RON2, *Pf*AMA1, *Pf*RON4, or *Pf*RhopH2. $AMA1_{83}$ is a proprotein form and $AMA1_{66}$ is a processed form.

Figure 6. *Pf*RON2 is expressed at the apical end of *Plasmodium* merozoites.

Schizont-infected erythrocytes and merozoites were dual-labeled with antisera against *Pf*RON2 and *Pf*AMA1 (A), *Pf*Clag3.1 (B), or *Pf*RON4 (C). Merged images are shown in the right panels. All segmented schizonts and merozoites are positive for *Pf*RON2. Nuclei are counterstained with DAPI. Colocalization of *Pf*RON2 with *Pf*RON4 (rhoptry neck marker) was observed but neither colocalized with *Pf*Clag3.1 (rhoptry body marker) nor *Pf*AMA1 (microneme marker). To eliminate the background staining, negative control sera were always used and images were assessed (data not shown).

Figure 7. Rhoptry neck localization of *Pf*RON2 by immunoelectron microscopy. Longitudinally sectioned merozoites in schizont-infected erythrocytes were labeled with anti-*Pf*RON2 serum followed by secondary Ab conjugated with gold particles. Gold particles were restricted to the narrow neck portion of the rhoptries (R). Two different images are shown (A and B). N indicates nucleus. Bars = 200 nm.

Figure 1.

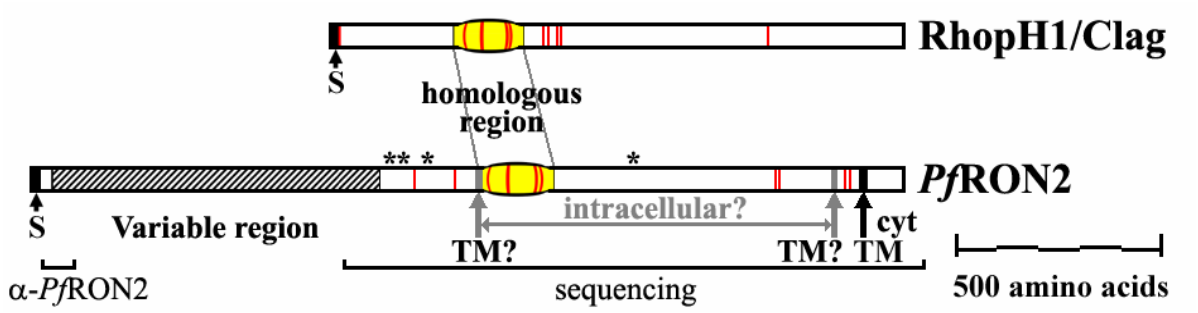
RhopH1/Clag
S
homologous region
** *
*
PfRON2
S
Variable region
intracellular?
TM?
TM?
TM
cyt
α-PfRON2
sequencing
500 amino acids

Figure 2.

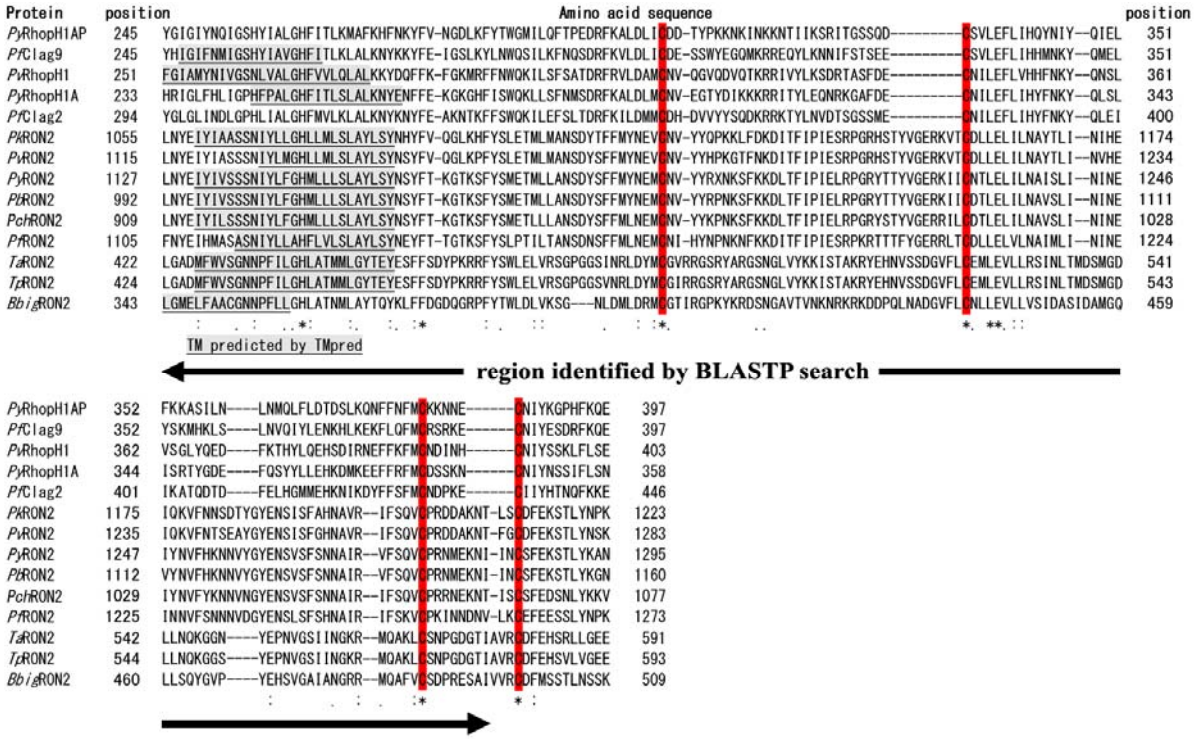
Protein
position
Amino acid sequence
position
PyRhopH1AP 245 YGIGIYNQIGSHYIALGHFITLKMAFKHFNKYFV-NGDLKFYTWGMILQFTPEDRFKALDLICDD-TYPKKNKINKKNTIIKSRITGSSQD---------GSVLEFLIHQYNIY--QIEL 351
PfClag9 245 YHIGIFNMIGSHYIAVGHFITLKLALKNYKKYFE-IGSLKYLNWQSILKFNQSDRFKVLDLICDE-SSWYEGQMKRREQYLKNNIFSTSEE---------GSVLEFLIHHMNKY--QMEL 351
PvRhopH1 251 FGIAMYNIVGSNLVALGHFVVLQLALKKYDQFFK-FGKMRFFNWQKILSFSATDRFRVLDAMCNV-QGVQDVQTKRRIVYLKSDRTASFDE---------GNILEFLVHHFNKY--QNSL 361
PyRhopH1A 233 HRIGLFHLIGPHFPALGHFITLSLALKNYENFFE-KGKGHFISWQKLLSFNMSDRFKALDLMCNV-EGTYDIKKKRRITYLEQNRKGAFDE---------GNILEFLIHYFNKY--QLSL 343
PfClag2 294 YGLGLINDLGPHLIALGHFMVLKLALKNYKNYFE-AKNTKFFSWQKILEFSLTDRFKILDMMCDH-DVVYYSQDKRRKTYLNVDTSGSSME---------GNILEFLIHYFNKY--QLEI 400
PkRON2 1055 LNYEIYIAASSNIYLLGHLLMLSLAYLSYNHYFV-QGLKHFYSLETMLMANSDYTFFMYNEVGNV-YYQPKKLFDKDITFIPIESRPGRHSTYVGERKVTGDLLELILNAYTLI--NIHE 1174
PvRON2 1115 LNYEIYIASSSNIYLMGHLLMLSLAYLSYNSYFV-QGLKPFYSLETMLMANSDYSFFMYNEVGNV-YYHPKGTFNKDITFIPIESRPGRHSTYVGERKVTGDLLELILNAYTLI--NVHE 1234
PyRON2 1127 LNYEIYIVSSSNIYLFGHMLLLSLAYLSYNSYFT-KGTKSFYSMETMLLANSDYSFFMYNEMGNV-YYRXNKSFKKDLTFIPIELRPGRYTTYVGERKIIGNTLELILNAISLI--NINE 1246
PbRON2 992 LNYEIYIVSSSNIYLFGHMLLLSLAYLSYNSYFT-KGTKSFYSMETMLLANSDYSFFMYNEMGNV-YYRPNKSFKKDLTFIPIELRPGRYTTYVGERKIIGDTLELILNAVSLI--NINE 1111
PchRON2 909 LNYEIYILSSSNIYLFGHMLLLSLAYLSYNSYFT-KGTKSFYSMETLLLANSDYSFFMLNEMGNV-YYKPNKSFKKDLTFIPIELRPGRYSTYVGERRILGDTLELILNAVSLI--NINE 1028
PfRON2 1105 FNYEIHMASASNIYLLAHFLVLSLAYLSYNEYFT-TGTKSFYSLPTILTANSDNSFFMLNEMGNI-HYNPNKNFKKDITFIPIESRPKRTTTFYGERRLTGDLLELVLNAIMLI--NINE 1224
TaRON2 422 LGADMFWVSGNNPFILGHLATMMLGYTEYESFFSDYPKRRFYSWLELVRSGPGGSINRLDYMCGVRRGSRYARGSNGLVYKKISTAKRYEHNVSSDGVFLGEMLEVLLRSINLTMDSMGD 541
TgRON2 424 LGADMFWVSGNNPFILGHLATMMLGYTEYESFFSDYPKRRFYSWLELVRSGPGGSVNRLDYMCGIRRGSRYARGSNGLVYKKISTAKRYEHNVSSDGVFLGEMLEVLLRSINLTMDSMGD 543
BbigRON2 343 LGMELFAACGNNPFLLGHLATNMLAYTQYKLFFDGDQGRPFYTWLDLVKSG----NLDMLDRMCGTIRGPKYKRDSNGAVTVNKNRKRKDDPQLNADGVFLGNLLEVLLVSIDASIDAMGQ 459
TM predicted by TMpred
region identified by BLASTP search
PyRhopH1AP 352 FKKASILN-----LNMQLFLDTDSLKQNFFNFMCKKNNE-------GNIYKGPHFKQE 397
PfClag9 352 YSKMHKLS-----LNVQIYLENKHLKEKFLQFMCRSRKE-------GNIYESDRFKQE 397
PvRhopH1 362 VSGLYQED-----FKTHYLQEHSDIRNEFFKFMCNDINH-------GNIYSSKLFLSE 403
PyRhopH1A 344 ISRTYGDE-----FQSYYLLEHKDMKEEFFRFMCDSSKN-------GNIYNSSIFLSN 358
PfClag2 401 IKATQDTD-----FELHGMMEHKNIKDYFFSFMCNDPKE-------GIIYHTNQFKKE 446
PkRON2 1175 IQKVFNNSDTYGYENSISFAHNAVR--IFSQVCPRDDAKNT-LSCDFEKSTLYNPK 1223
PvRON2 1235 IQKVFNTSEAYGYENSISFGHNAVR--IFSQVCPRDDAKNT-FGCDFEKSTLYNSK 1283
PyRON2 1247 IYNVFHKNNVYGYENSVSFSNNAIR--VFSQVCPRNMEKNI-INCSFEKSTLYKAN 1295
PbRON2 1112 VYNVFHKNNVYGYENSVSFSNNAIR--VFSQVCPRNMEKNI-INCSFEKSTLYKGN 1160
PchRON2 1029 IYNVFYKNNVNGYENSVSFSNNAIR--IFSQVCPRRNEKNT-ISCSFEDSNLYKKV 1077
PfRON2 1225 INNVFSNNNVDGYENSLSFSHNAIR--IFSKVCPKINNDNV-LKCEFEESSLYNPK 1273
TaRON2 542 LLNQKGGN-----YEPNVGSIINGKR--MQAKLCSNPGDGTIAVRCDFEHSRLLGEE 591
TgRON2 544 LLNQKGGS-----YEPNVGSIINGKR--MQAKLCSNPGDGTIAVRCDFEHSVLVGEE 593
BbigRON2 460 LLSQYGVP-----YEHSVGAIANGRR--MQAFVCSDPRESAIVVRCDFMSSTLNSSK 509

Figure 3.

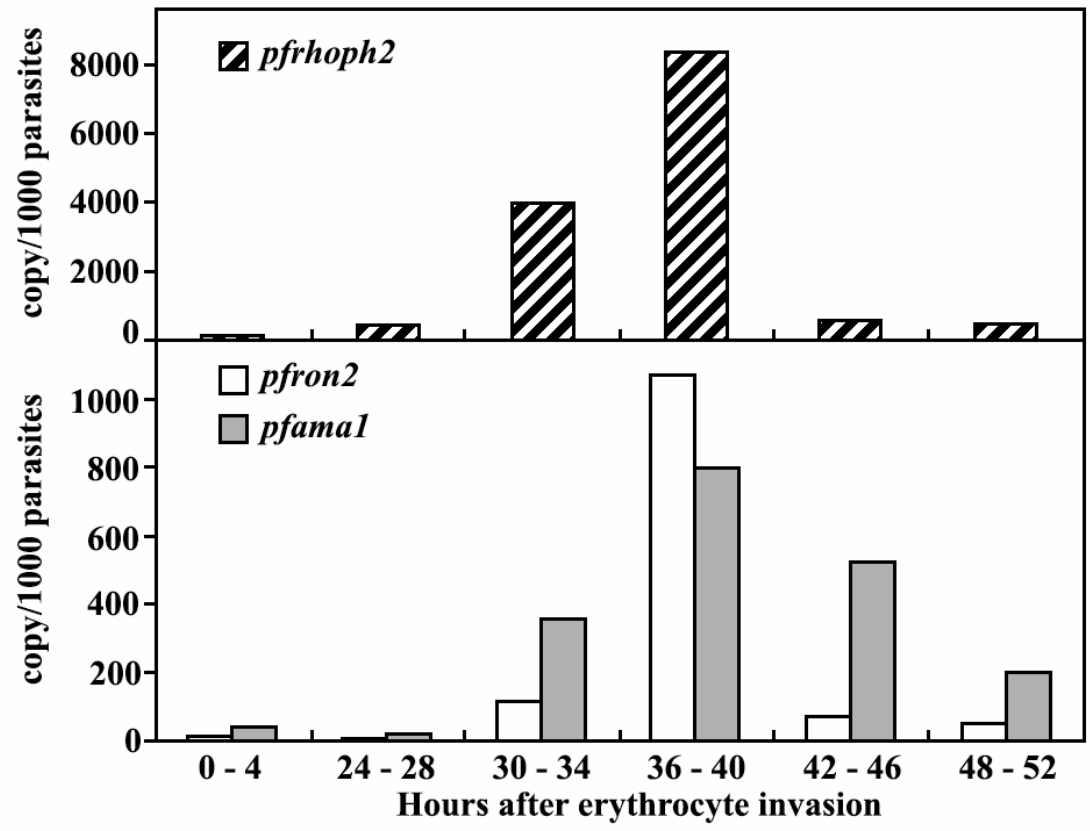
pfrhoph2
copy/1000 parasites
8000
6000
4000
2000
0
pfron2
pfama1
copy/1000 parasites
1000
800
600
400
200
0
0 - 4
24 - 28
30 - 34
36 - 40
42 - 46
48 - 52
Hours after erythrocyte invasion

Figure 4.

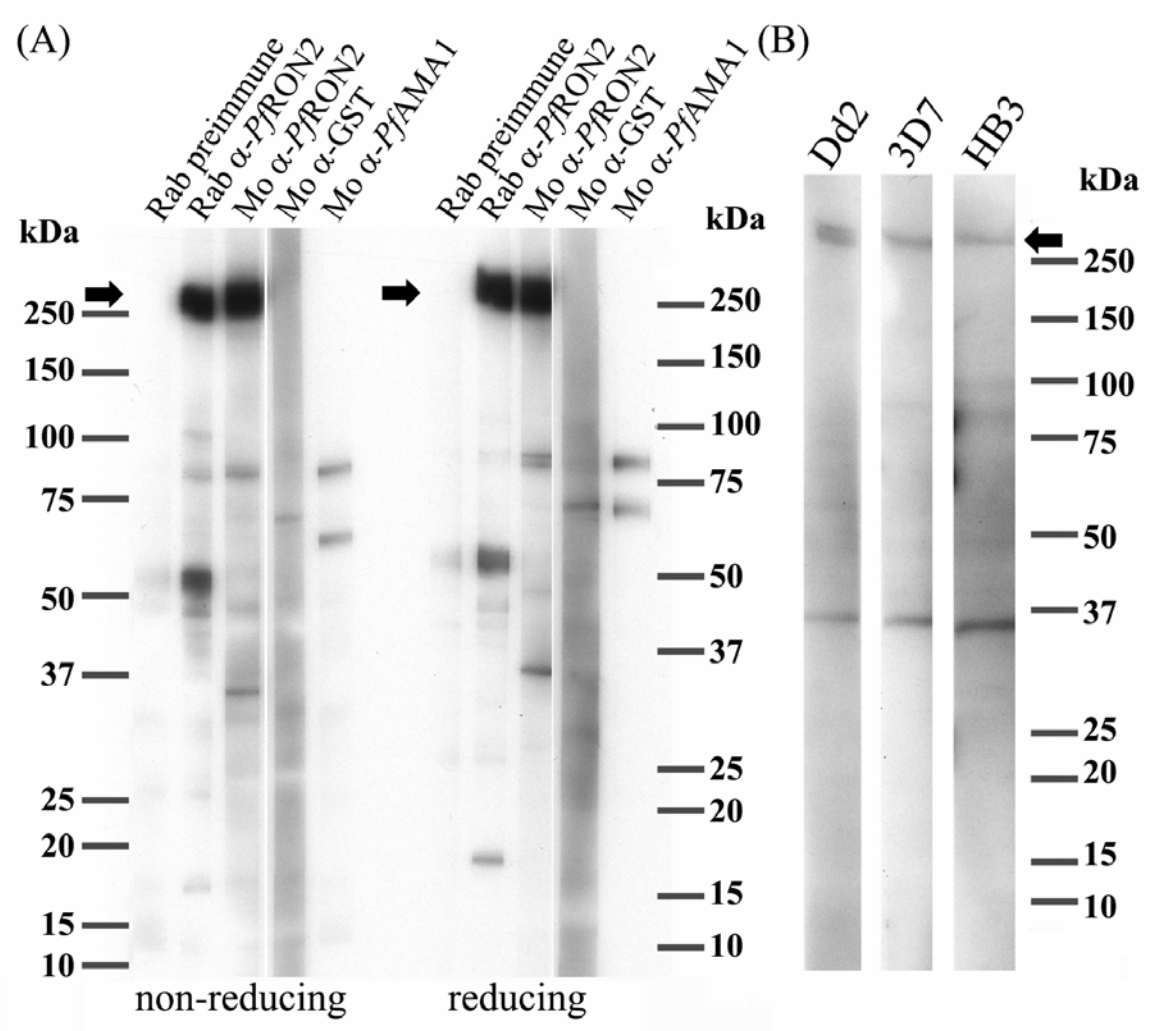
(A)
Rab preimmune
Rab α-PfRON2
Mo α-PfRON2
Mo α-GST
Mo α-PfAMA1
kDa
250
150
100
75
50
37
25
20
15
10
non-reducing
reducing
(B)
Dd2
3D7
HB3
kDa

Figure 5.

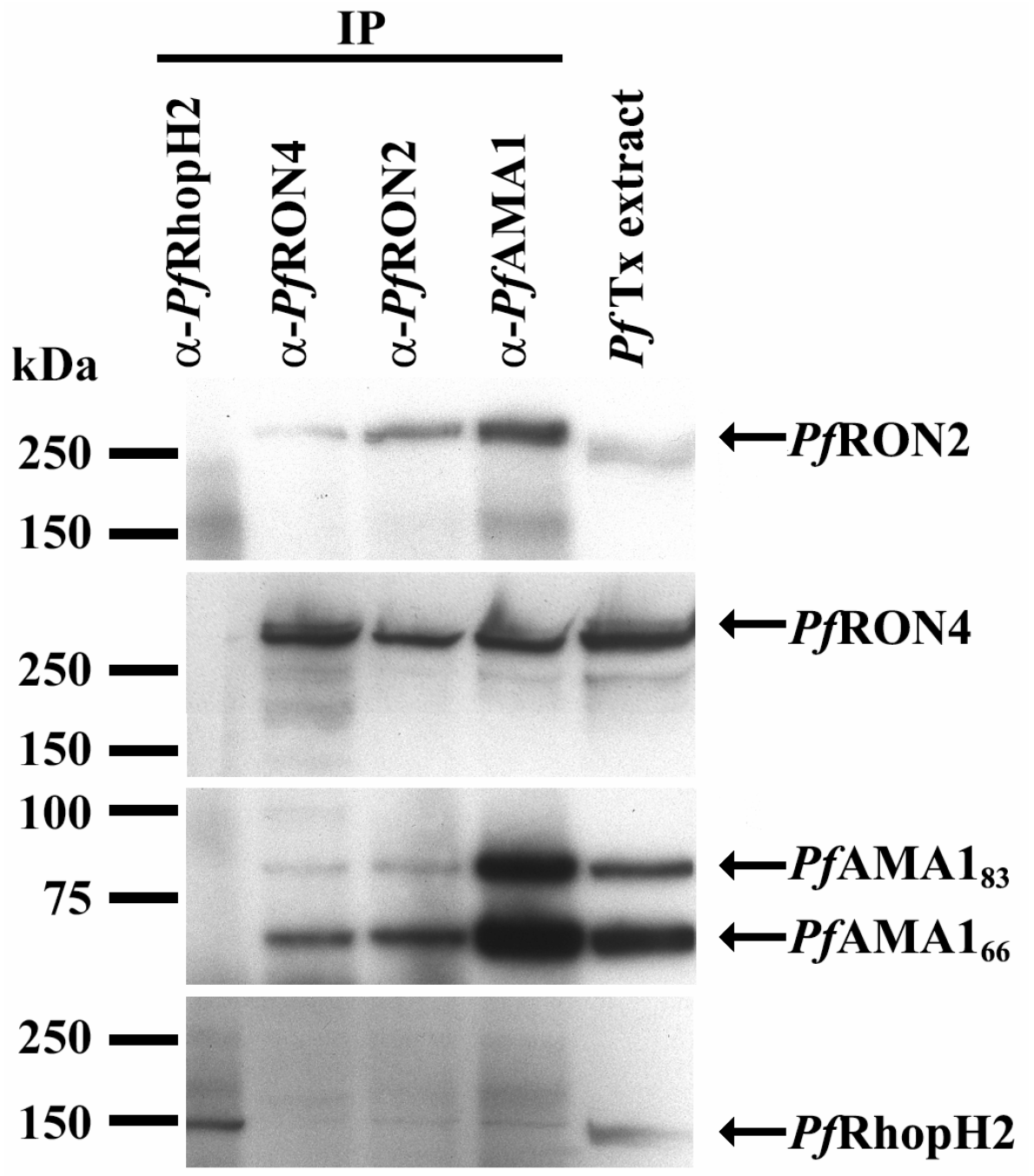
IP
α-PfRhopH2
α-PfRON4
α-PfRON2
α-PfAMA1
Pf Tx extract
kDa
250
150
PfRON2
250
150
PfRON4
100
75
PfAMA1 83
PfAMA1 66
250
150
PfRhopH2

Figure 6.

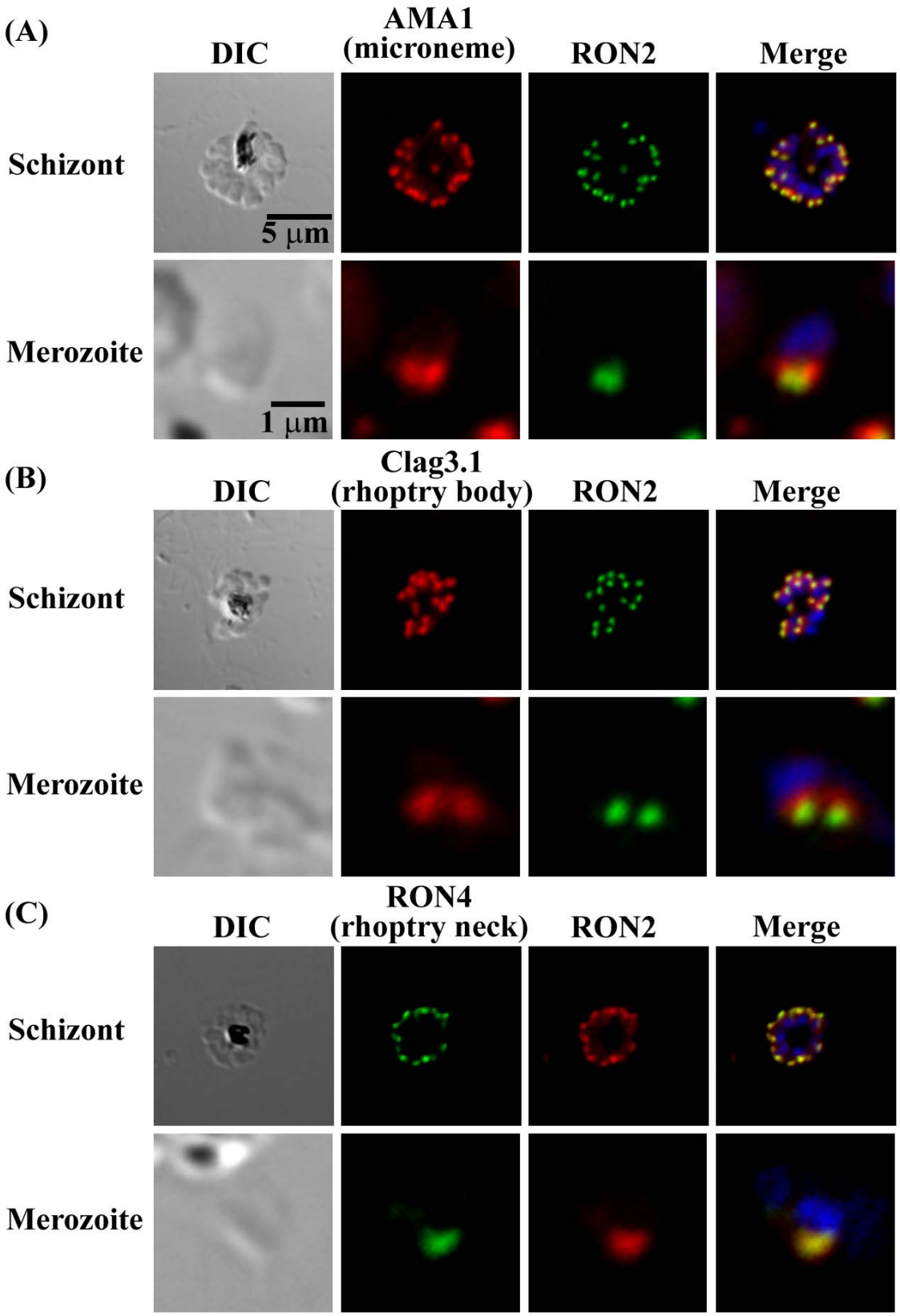
(A)
DIC
AMA1 (microneme)
RON2
Merge
Schizont
5 μm
Merozoite
1 μm
(B)
DIC
Clag3.1 (rhoptry body)
RON2
Merge
Schizont
Merozoite
(C)
DIC
RON4 (rhoptry neck)
RON2
Merge
Schizont
Merozoite

Figure 7.